Predictive simulation of nonlinear ultrasonics

Yanfeng Shen, Victor Giurgiutiu
Department of Mechanical Engineering, University of South Carolina, Columbia, SC 29208

ABSTRACT

Most of the nonlinear ultrasonic studies to date have been experimental, but few theoretical predictive studies exist, especially for Lamb wave ultrasonic. Compared with nonlinear bulk waves and Rayleigh waves, nonlinear Lamb waves for structural health monitoring become more challenging due to their multi-mode dispersive features. In this paper, predictive study of nonlinear Lamb waves is done with finite element simulation. A pitch-catch method is used to interrogate a plate with a "breathing crack" which opens and closes under tension and compression. Piezoelectric wafer active sensors (PWAS) used as transmitter and receiver are modeled with coupled field elements. The "breathing crack" is simulated via "element birth and death" technique. The ultrasonic waves generated by the transmitter PWAS propagate into the structure, interact with the "breathing crack", acquire nonlinear features, and are picked up by the receiver PWAS. The features of the wave packets at the receiver PWAS are studied and discussed. The received signal is processed with Fast Fourier Transform to show the higher harmonics nonlinear characteristics. A baseline free damage index is introduced to assess the presence and the severity of the crack. The paper finishes with summary, conclusions, and suggestions for future work.

Keywords: nonlinear ultrasonics, nonlinear Lamb waves, finite element simulation, "element birth and death", structural health monitoring (SHM), nondestructive evaluation (NDE), piezoelectric wafer active sensors (PWAS), damage detection.

1. INTRODUCTION

Structural health monitoring during the early stage of material degradation is important for detecting micro cracks that are precursors to structural damage. Conventional linear elastic ultrasonic techniques are sensitive to gross defects but less sensitive to micro cracks. The nonlinear ultrasonic technique, which uses distinctive higher harmonics and sub harmonics features, proves itself a promising approach to detect micro cracks and other incipient damage [1, 2, 3, 4].

The combined use of guided Lamb waves and nonlinear methods are of interest because they combine the sensitivity of nonlinear methods with large inspection ranges of guided waves. To date, most studies on nonlinear ultrasonics have been experimental, and generally using non-dispersive waves like longitudinal bulk waves or Rayleigh waves[5, 6, 7]. Experimental studies of nonlinear Lamb waves have been carried out recently, demonstrating the capability of nonlinear Lamb wave to detect structural defects[8, 9, 10]. Generation of higher harmonics Lamb waves have been investigated theoretically[11, 12], and existence of anti-symmetric or symmetric Lamb waves at nonlinear higher harmonics has been discussed via modal analysis approach and the method of perturbation. However, these theoretical studies considered only the simple case where nonlinearity is present over the whole domain of the material; other causes for nonlinear behavior, such as localized material degradation or micro cracks, have not been investigated theoretically due to the mathematical complexity. In this paper, we study the breathing crack nonlinearity using the finite element method (FEM). A breathing crack will introduce nonlinearity into the structure by varying structural stiffness between opening and closing. Experimental work on using nonlinear Lamb waves for evaluating micro fatigue cracks have been conducted[13, 14, 15], and the results show its good potential for detecting structural micro-cracks. Regarding finite element simulation of cracked structural components, most studies have been on nonlinear vibrations[16, 17]; a few studies on longitudinal bulk wave nonlinear effects also exist[18, 19]. Most of the numerical studies use the modeling of a breathing crack by the contact model. However, the contact model requires prior experience for defining the contact pairs and proper calculation parameters such as contact stiffness, friction, etc.

In this paper, predictive simulation of nonlinear Lamb waves interrogating a cracked plate is carried out. Piezoelectric wafer active sensors (PWAS) are used to construct pitch-catch pairs[20]; they are modeled with coupled field elements. An "element birth and death" approach is used to model the closing and opening of the crack. The crack presence and severity is indicated by the distinctive nonlinear higher harmonics, which are briefly discussed next.

2. GENERATION OF HIGHER HARMONICS THROUGH NONLINEAR MATERIAL PROPERTIES

The nonlinear behavior in vibrations and waves has been studied and discussed by several researchers[21, 22, 23, 24]; the phenomenon of higher harmonic generation can be explained by the nonlinearity in the elastic behavior of materials, which means the relationship between stress σ and strain ε is nonlinear as shown in Figure 1.

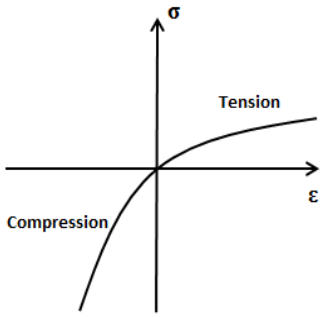

Figure 1. Nonlinear relationship between stress and strain[1]

The corresponding nonlinear version of Hooke's law can be expressed as[25]

$$\sigma = E\varepsilon(1+\beta\varepsilon+\gamma\varepsilon^2+\cdots) \tag{1}$$

Where, E is Young's modulus, while β and γ are the 2nd and 3rd nonlinear elastic coefficients. In order to explain the generation of higher order harmonics, consider a nonlinear dynamic system of the form

$$U = Ax(1+\beta x+\gamma x^2+\cdots) \tag{2}$$

Where U is the general output of the system, x is the general input of the system, A is a scale factor, and β, γ are the 2nd and 3rd nonlinear coefficients. Consider a harmonic input:

$$x(\omega) = \hat{x}e^{i\omega t} \tag{3}$$

By substituting (3) into (2), the output of the nonlinear system takes the form

$$\begin{aligned} U &= A\hat{x}e^{i\omega t} + A\beta(\hat{x}e^{i\omega t})^2 + A\gamma(\hat{x}e^{i\omega t})^3 + \cdots \\ &= A\hat{x}e^{i\omega t} + A\beta\hat{x}\hat{x}e^{i2\omega t} + A\gamma\hat{x}^2\hat{x}e^{i3\omega t} + \cdots \\ &= Ax(\omega) + A\beta\hat{x}\cdot x(2\omega) + A\gamma\hat{x}^2\cdot x(3\omega) + \cdots \end{aligned} \tag{4}$$

Equation (4) shows that the output of the nonlinear system contains higher order harmonics $2\omega, 3\omega\cdots$, while the input to the system contains only one frequency component ω. This distinctive feature allows us to reveal the material degradation, fatigue or micro cracks, which introduce nonlinearity to structures.

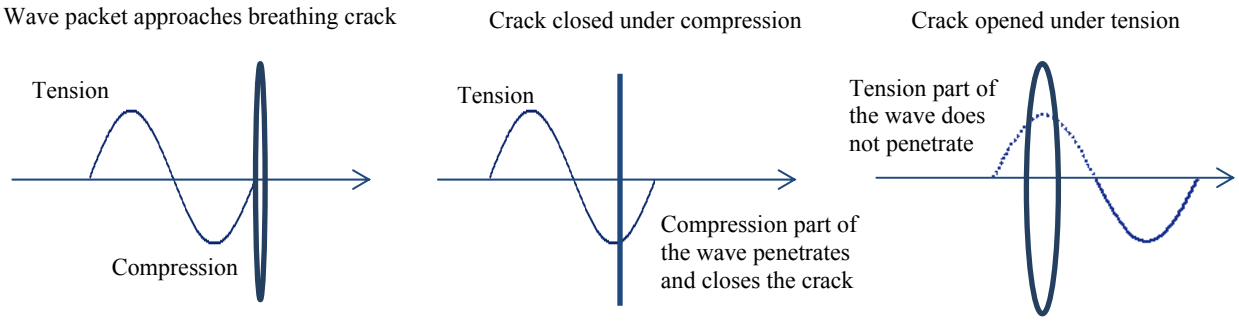

Figure 2. Ultrasonic waves propagating through a breathing crack

When large amplitude ultrasonic waves reach a breathing crack, the crack will be opened and closed under tension and compression, with the compression part of the waves penetrating the crack, while the tension part cannot, as shown in Figure 2. The nonlinear phenomenon lies in the fact that the apparent local stiffness of the crack region changes under tensile and compression. When the compressional part of the waves reaches the crack, the crack will be closed and the ultrasonic wave penetrates the crack like propagating through continuous medium. Under stretching, the crack opens, and the material becomes discontinuous resulting in a decreased local stiffness[26]. The incident waves, after interacting with the breathing crack, will pick up higher harmonics due to this local nonlinearity.

3. THE "ELEMENT BIRTH AND DEATH" APPROACH

We propose to use the "element birth and death"[27] approach to simulate the dynamic behavior of a structure with breathing cracks. This approach has been previously used in applications in which one can easily identify elements that are activated and then deactivated[28].

"Element birth and death" technique could be described as deactivating and reactivating selected elements according to certain criteria. To achieve the "element death" effect, the selected elements are deactivated by multiplying their stiffness matrices by a severe reduction factor, η (usually 1E-6 or smaller), while mass, damping, loads and other such effects are set to zero. Thus, upon deactivation, the element stiffness matrix, mass matrix and associated loads will no longer contribute to the assembled global matrices. It should be noted that, through this approach, the "dead" elements are not removed from the model, but left in place in a dormant state with a greatly diminished participation. Similarly, when elements are "born", they are not added to the model. Instead, the dormant elements are simply reactivated, recovering their original stiffness, mass, damping, element loads, etc. The element equation of a certain selected element before and after deactivation in a dynamic problem could be expressed as

Original element equation
$$[M^e]\{\ddot{U}^e\}+[C^e]\{\dot{U}^e\}+[K^e]\{U^e\}=\{Q^e\} \tag{5}$$

Deactivated element equation
$$[\Phi]\{\ddot{U}^e\}+[\Phi]\{\dot{U}^e\}+\eta[K^e]\{U^e\}=\{\Phi\} \tag{6}$$

Where M^e, C^e, K^e, Q^e are the element mass matrix, damping matrix, stiffness matrix and external loads. The reduction factor η is very small ($\eta << 1$, typically $\eta < 1E-6$). And the symbol Φ denotes a zero matrix or vector. The assembled global equation will take the form

Original global equation
$$\begin{pmatrix} M_{11} & \cdots & 0 \\ \vdots & +M^e & \vdots \\ 0 & \cdots & M_{nn} \end{pmatrix}\begin{Bmatrix} \ddot{u}_1 \\ \vdots \\ \ddot{u}_n \end{Bmatrix}+\begin{pmatrix} C_{11} & \cdots & 0 \\ \vdots & +C^e & \vdots \\ 0 & \cdots & C_{nn} \end{pmatrix}\begin{Bmatrix} \dot{u}_1 \\ \vdots \\ \dot{u}_n \end{Bmatrix}+\begin{pmatrix} K_{11} & \cdots & 0 \\ \vdots & +K^e & \vdots \\ 0 & \cdots & K_{nn} \end{pmatrix}\begin{Bmatrix} u_1 \\ \vdots \\ u_n \end{Bmatrix}=\begin{Bmatrix} Q_1 \\ \vdots+Q^e \\ Q_n \end{Bmatrix} \tag{7}$$

Deactivated global equation
$$\begin{pmatrix} M_{11} & \cdots & 0 \\ \vdots & +\Phi & \vdots \\ 0 & \cdots & M_{nn} \end{pmatrix}\begin{Bmatrix} \ddot{u}_1 \\ \vdots \\ \ddot{u}_n \end{Bmatrix}+\begin{pmatrix} C_{11} & \cdots & 0 \\ \vdots & +\Phi & \vdots \\ 0 & \cdots & C_{nn} \end{pmatrix}\begin{Bmatrix} \dot{u}_1 \\ \vdots \\ \dot{u}_n \end{Bmatrix}+\begin{pmatrix} K_{11} & \cdots & 0 \\ \vdots & +\eta K^e & \vdots \\ 0 & \cdots & K_{nn} \end{pmatrix}\begin{Bmatrix} u_1 \\ \vdots \\ u_n \end{Bmatrix}=\begin{Bmatrix} Q_1 \\ \vdots+\Phi \\ Q_n \end{Bmatrix} \tag{8}$$

Comparing equation (8) with (7), we see that the elements after deactivation, will no longer contribute to the structure because $\eta K^e \approx [\Phi]$ with $\eta << 1$. The nonlinear effect is imparted by the periodic changing of matrices M, C and K.

To model the breathing crack, we use a very thin layer of nonlinear element. A typical mesh of the crack zone is shown in Figure 3 (a). When a certain condition is met, for example when elements are under tension, they are deactivated. Then, the stiffness, mass, damping, etc. of this thin layer of elements' stiffness, mass, damping, etc. will not contribute to the global matrices, and the crack is considered open. We say that the elements are "dead", i.e., inactive. Likewise, when the elements are under compression, the elements are "born", i.e., reactivated, and their stiffness, mass, damping, etc. will recover to their original value contributing again to the structure. In this case, the structure behaves like a continuum, and the crack is considered closed. The crack opening or closing status is judged for every calculation step in the transient analysis; calculation configuration of the current step is based on the calculation results of the previous step. For instance, at the first calculation step, when no wave propagating in the structure, the crack is considered open. Hence

calculation configuration of the current step is "crack-open" status with the selected layer of elements deactivated. After the calculation, the results of this step is used to judge whether the crack is closed or not and determine calculation configuration for the next step. If the crack is closed, then the elements are reactivated for the next step, so on and so forth. In practice, for each step, all the selected elements are deactivated at the beginning, then it will be judged whether they should be reactivated or stay deactivated.

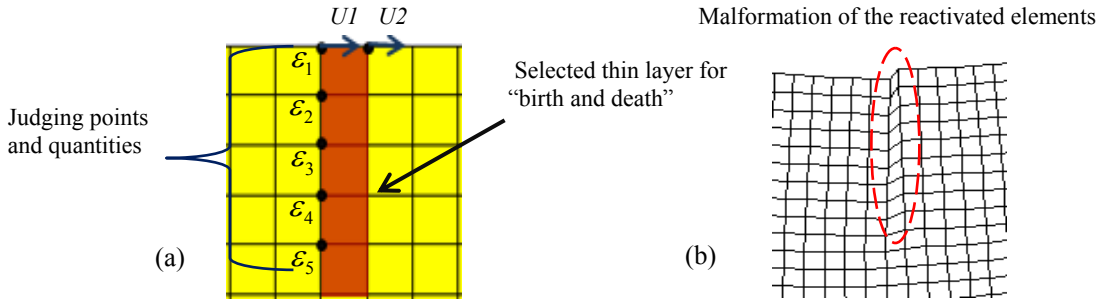

Figure 3. (a) crack status judgment quantities; (b) malformation of the reactivated elements

The selection of the appropriate "crack status" criterion plays an important role in this simulation work. For the purpose of simulating a breathing crack with "element birth and death" technique, a "crack status" criterion is developed based on the physical interpretation of the model.

An intuitive idea is to compare the displacements of the two nodes located on the two edges of the selected elements as shown in Figure 3. The element strain in x direction could be approximated by:

$$\varepsilon_x = \frac{U2 - U1}{L} \tag{9}$$

Where $U1$ and $U2$ are the displacements of the two nodes located on the two edges of the selected element, and L is the element size in x direction. When $\varepsilon_x \geq 0$, the crack is under tension, the two corresponding physical particles on the two side of the crack move apart from each other, and the crack is opened, indicating that the elements should stay deactivated. When $\varepsilon_x < 0$, the crack is under compression, the corresponding physical particles on the two sides of the crack move nearer to each other, and the crack is closed, indicating that the elements should be reactivated.

This criterion seems reasonable; however, in practice, it turns out that this condition is not strong enough to render a good crack open and close behavior. Numerical experiments with this criterion have shown that after several open and close cycles, the crack could not be opened as expected. The reason behind this phenomenon is that the finite element transient analysis works on a discretized time basis. After the deactivation, the thin layer of element stiffness, mass, etc. becomes so weak, that they will undergo relatively big deformation, which may make the distance between the two opposing two nodes very small under compression. Then the criterion states that the crack should be closed, and the elements are reactivated, but they are "born with malformation" shown if Figure 3 (b), which means the elements no longer take the original rectangular shape but a deformed shape. Even under tension, the distance between the two nodes stays still smaller than the element size, and this situation will never satisfy the open criterion again.

To solve this issue, an averaged nodal strain $\bar{\varepsilon}_x$ in the front of the selected elements is selected to evaluate the crack open condition. Thus, even though the newly "born" elements may suffer malformation, as soon as they are under tension, indicated by $\bar{\varepsilon}_x > 0$, they will become deactivated and the crack will open. As mentioned before, for each step, the selected elements are first deactivated, then they are judged by the criterion whether they should be activated or not. So the reactivation (crack close) criterion could be concluded as

$$(U2 - U1 < 0) \cap (\bar{\varepsilon}_x = \frac{\sum_1^n \varepsilon_n}{n} < 0) \tag{10}$$

Since the judgment for a certain step is based on the calculation result previous step, the $\bar{\varepsilon}_x$ is obtained from the front nodes of selected element, which could, to some degree, compensate for the small time delay and theoretically achieve a better accuracy. The result is also considered more accurate if the malformation is not severe, so a small time step is expected to reduce the malformation of newly "born" elements.

4. FINITE ELEMENT MODEL

In our model (Figure 4), four $7\text{mm} \times 7\text{mm} \times 0.2\text{mm}$ piezoelectric wafer active sensors (PWAS) are considered bonded on a 2-mm thick aluminum plate. One PWAS works as a transmitter and sends tone burst excitation signal into the structure; the other three PWAS transducers function as receivers and detect the wave signal arriving in sequence at the three locations. The plate is long enough to ensure the received signals are not influenced by boundary reflections. The distances between the transmitter PWAS and the receiver PWAS transducers are shown in Figure 4. The crack is located at 200 mm from the transmitter, such that the S0 and A0 wave packets have already separated when Lamb wave arrives at the crack location; hence the S0 and A0 wave packets interact with the breathing crack individually, which allows us to see how the crack influences differently the S0 and A0 waves.

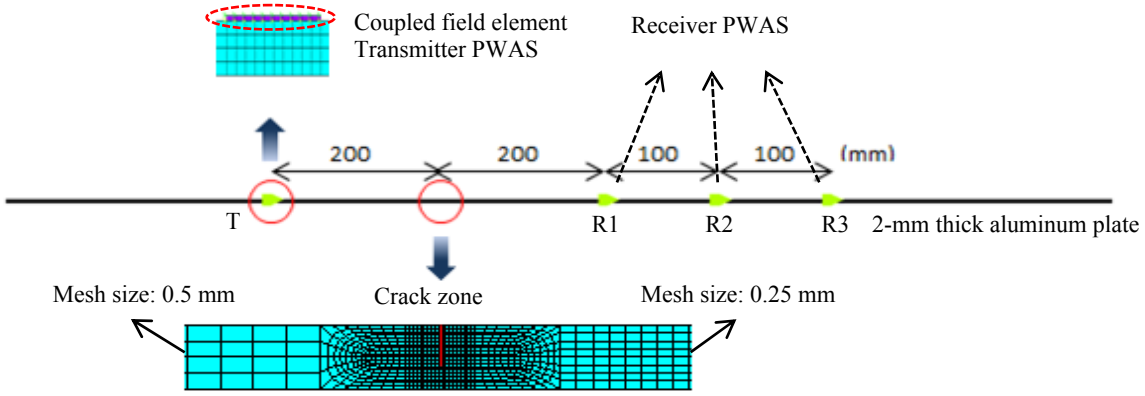

Figure 4. Finite Element Model

A 2D transient finite element model is built under the plane strain assumption to simulate a pitch-catch SHM process interrogating a cracked plate. The PWAS transducers are modeled with coupled field elements (PLANE13) which couple the electrical and mechanical variables (ANSYS 13.0 Multi-Physics). The plate is modeled with four nodes structure element PLANE182 with "element birth and death" capability. A 100-volts 5-counts Hanning-window modulated tone burst signal centered at 100 kHz is applied on the top electrode of the transmitter PWAS. The plate is under free boundary condition. The Lamb wave sent out by transmitter PWAS will propagate along the plate, interact with the breathing crack, pick up nonlinear features, and be detected by the receiver PWAS.

To solve this problem with good accuracy and high efficiency, a meshing strategy of varying mesh density needs to be performed. In general, a denser mesh will render a more accurate result, but will also consume more computer resource and calculation time. The maximum element size and time step to ensure accuracy is selected[29]

$$l_e = \frac{\lambda_{min}}{20} \tag{11}$$

$$\Delta t = \frac{1}{20 f_{max}} \tag{12}$$

The frequency spectrum for the 5-count tone burst excitation signal lies in the range $0 < f < 200\,\text{kHz}$ as shown in Figure 5. For a 100 kHz wave, a mesh size of 1.25 mm and a time step of 0.25 microseconds are enough according to Equations (11) and (12) to ensure accuracy; hence, a fundamental mesh size of 0.5 mm is adopted between the transmitter and the crack. Since the mechanical response at crack zone is very complicated, the crack zone is more densely meshed with much smaller elements. A very thin layer of elements at the crack zone are selected to be deactivated or reactivated. The thinner the layer is, the more accurate the simulated crack will be. After interacting with the breathing crack, the Lamb waves will pick up higher frequency components. To ensure the accuracy of higher harmonics, a mesh size of 0.25 mm

is adopted between the crack zone and the receivers, which is $1/5$ of 1.25 mm. The varying density mesh strategy is shown in Figure 4. The time step of 0.125 microseconds is adopted, which is $1/2$ of 0.25 microseconds. Both the selected mesh size and time step ensure that the 2nd harmonic is accurately modeled in frequency domain.

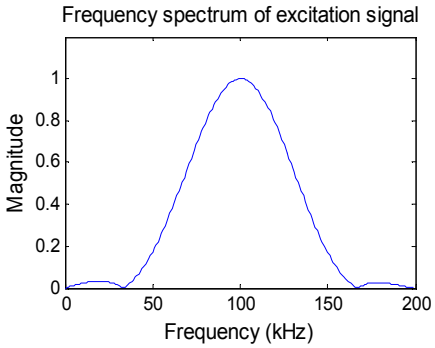

Figure 5. Frequency spectrum of excitation signal

The severity of damage is represented by the number of elements selected to be deactivated and reactivated. We define the damage severity as the index where $r = a/h$ (a and h are the crack size and plate thickness respectively). An index of $r = 0.0$ corresponds to pristine condition, where there is no crack in the plate. In our simulation, we used 20 elements across the thickness at the crack zone. Different damage severities r =0.6, 0.5, 0.4, 0.3, 0.2, 0.1 and 0.0 were generated by selecting 12, 10, 8, 6, 4, 2 and 0 elements.

ANSYS uses an average nodal solution for data post-processing. Hence, the deactivated elements must be excluded from the averaged process to avoid contamination of the results. For each calculation step, an index is recorded to indicate if the selected elements are deactivated or reactivated. If the elements are deactivated, then they will be un-selected for the final average nodal value post-processing to avoid contamination.

5. SIMULATION RESULTS AND DISCUSSION

As mentioned in the previous section, simulations of different damage severity cases were carried out with r =0.6, 0.5, 0.4, 0.3, 0.2, 0.1 and 0.0. For $r = 0.6$, the nonlinear effect should be the most obvious, therefore this case was used as most representative for nonlinear effect. It was observed that the breathing crack behaves well: when tension part of the Lamb wave arrives at the crack, it opens; while compression part of the Lamb wave arrives, it closes. The situations of crack open and close for both S0 and A0 modes are shown in Figure 6.

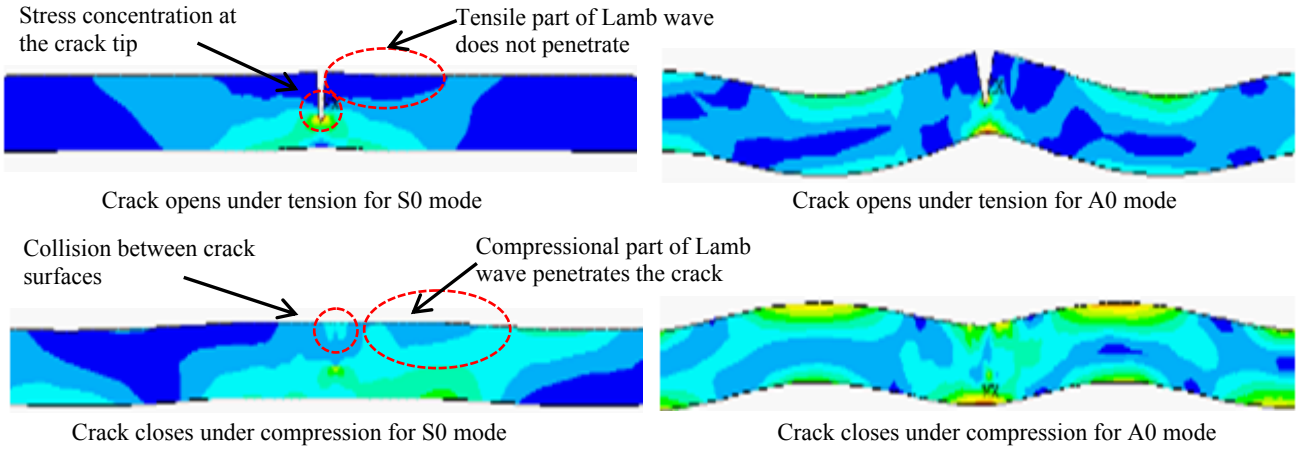

Figure 6. Breathing crack opens and closes for S0 and A0 modes ($r = 0.6$)

It can be observed that the breathing crack behaves well with respect to open and close for both S0 and A0 modes. Under tension, the crack opens, and stress concentration could be observed at the crack tip; it is apparent that the tension part of the Lamb wave does not penetrate the crack. When the compression part of the Lamb wave arrives, the crack closes, and collision between "crack surfaces" is noticed; hence, the compression part of the Lamb wave can penetrate into the crack.

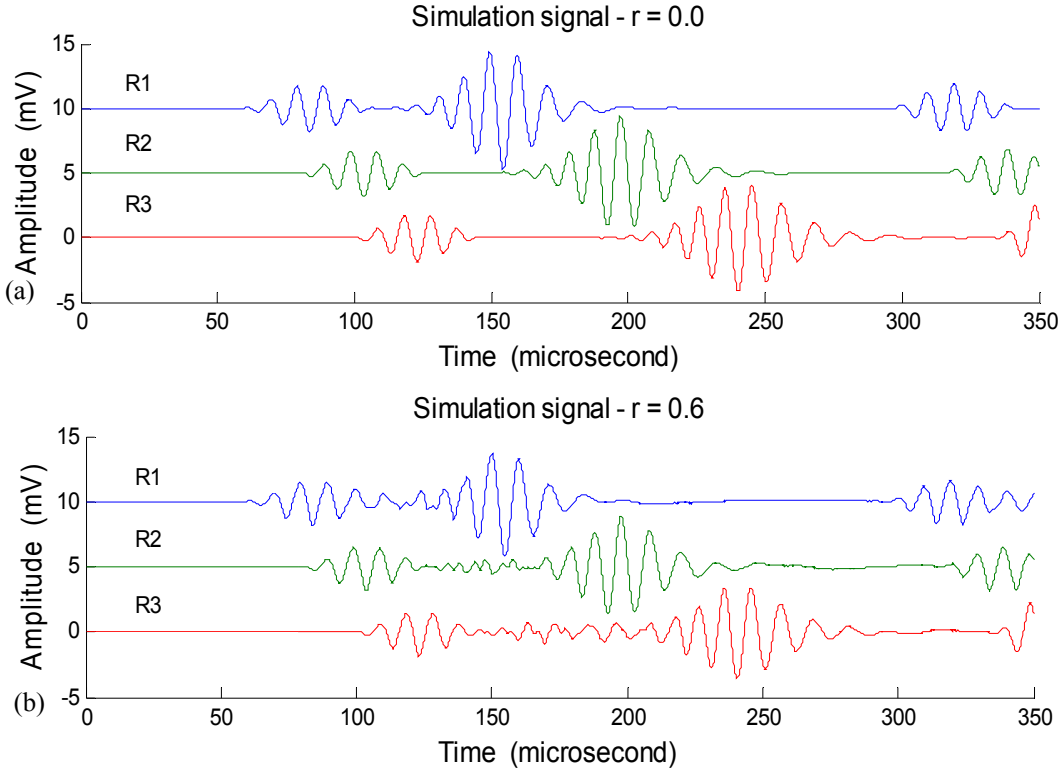

Figure 7. Time domain simulation signal for (a) pristine plate with r = 0.0 and (b) cracked plate with r = 0.6

The time domain signal picked up by the three PWAS receivers is shown in Figure 7 (a) for pristine case (r =0.0) and in Figure 7 (b) for cracked case (r =0.6).

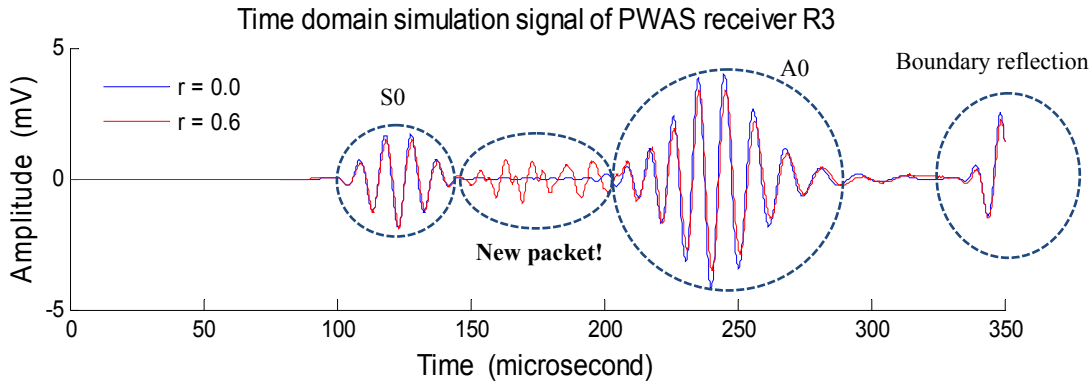

Figure 8. Superposed time domain simulation signals at PWAS receiver R3 for pristine (r = 0) and cracked (r = 0.6) cases

The superposed time domain simulation signal for PWAS receiver R3 are shown in Figure 8. It can be observed from Figure 8, that compared with pristine condition, the cracked plate signal has a slight amplitude drop and phase shift in both S0 and A0 packets. Another difference is that a new wave packet appears due to the breathing crack. This new packet is a special feature introduced by the breathing crack. Figure 7 shows that the new packet spreads out as it propagates, meaning it is dispersive. This new packet may be introduced by mode conversion at the breathing crack:

when the crack opens, no matter if by the S0 and A0 packet, the effect of tension force at the cracked location could be decomposed into stretching and bending w.r.t the neutral axis, which will generate correspondingly S0 and A0 components. When the crack closes, since the crack surfaces may have relative velocity, collision between the crack surfaces will happen. The effect of this collision could also be decomposed into two parts: compression and bending, which will generate respectively S0 and A0 components. The nonlinear effect will also introduce higher harmonics components in both S0 and A0; since both modes are dispersive, the new packet feature indicated in Figure 8 could also come from the high frequency components which "escaped" and separated from the S0 and A0 packets. Thus, it could be deduced that the new packet feature comes from the breathing crack, and contains both S0 and A0 waves. Fourier transforms of S0, A0 and the new wave packets are carried out, and plotted in Figure 9.

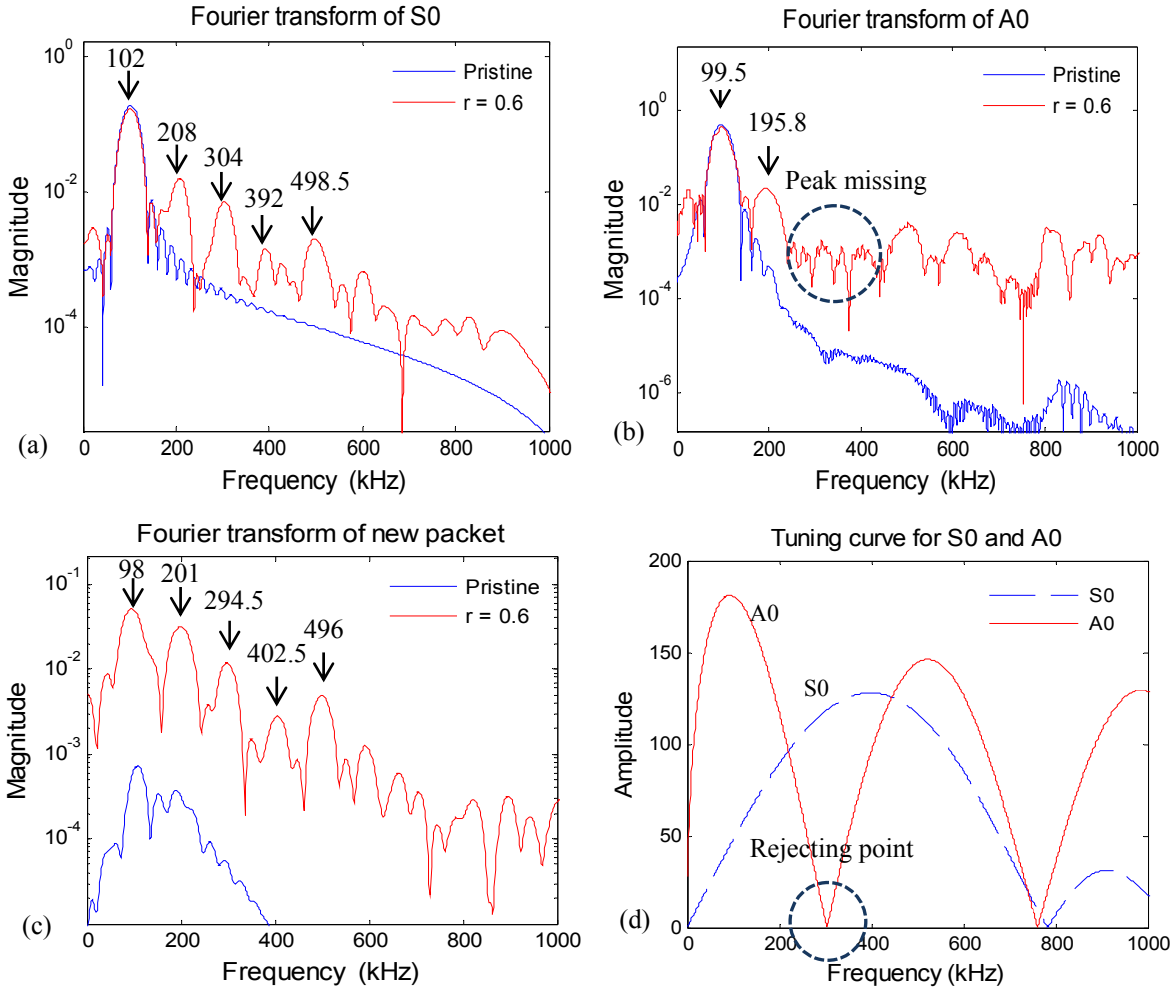

Figure 9. Fourier transform of S0, A0 and the new component: (a) S0; (b) A0; (c) new packet; (d) tuning curves for A0 and S0

For all the wave packets, the pristine signal does not shown any higher frequency components whereas the signal from cracked plate shows distinctive nonlinear higher harmonics. Figure 9a shows distinctive nonlinear higher harmonics in the S0 wave packet. Since the excitation frequency is centered at $f_c = 100$ kHz, the 102 kHz peak corresponds to the excitation frequency f_c, and the 208 kHz, 304 kHz, 392 kHz and 498.5 kHz correspond to $2f_c, 3f_c, 4f_c$ respectively. For the A0 wave packet (Figure 9b), the first peak corresponds to the excitation frequency f_c, and the second harmonic $2f_c$ could be clearly observed at 195.8 kHz, but the third harmonic $3f_c$ is somehow missing. This phenomenon is due to the tuning effect of PWAS[29]. The tuning curve shown in Figure 9d indicates that at around 300 kHz, which is where the third harmonic should appear, the A0 mode reaches its rejection point; In other words, for the given PWAS and plate structure, this frequency could not be detected due to the rejection effect at the receiver PWAS. However, the second

nonlinear higher harmonic is clearly detected. Analysis of the observed "new packet" (Figure 8c) also reveals the nonlinear higher harmonics pattern. The peaks correspond to excitation frequency f_c, nonlinear higher harmonics $2f_c, 3f_c, 4f_c$ and $5f_c$. In this new packet, the feature of nonlinear higher harmonics seems to be more obvious than in the S0 and A0 packets. And the amplitudes of the higher harmonics are closer to that of the excitation.

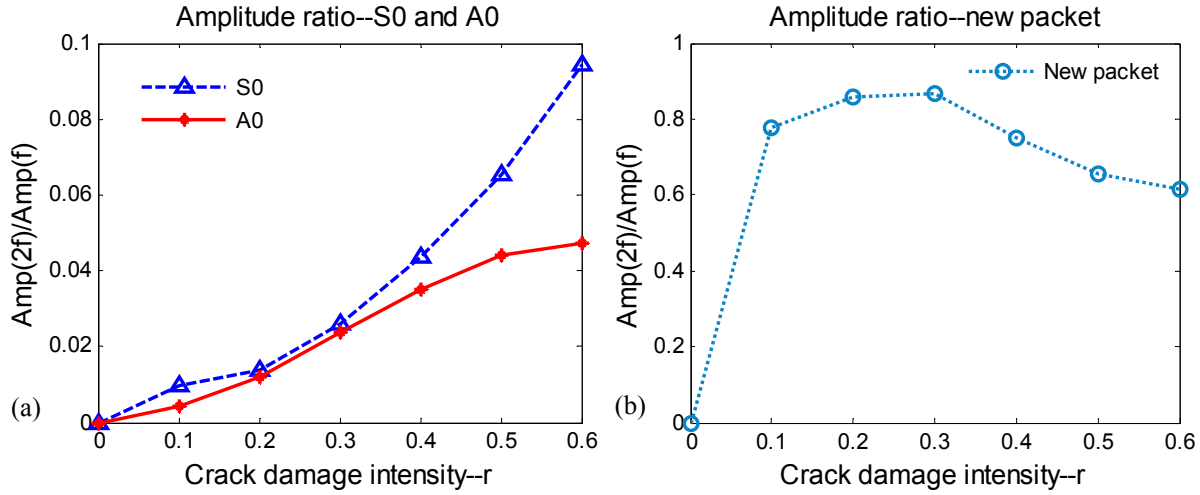

Figure 10. Damage severity index

To further identify the damage severity, the simulation results from r = 0.6, 0.5, 0.4, 0.3, 0.2, 0.1 and 0.0 are compared. The amplitude ratio of second harmonic to excitation frequency is adopted to show the degree of nonlinear effect, which may serve as a damage index indicating damage severity, i.e.

$$DI = \frac{A(2f_c)}{A(f_c)} \tag{13}$$

Where $A(f_c)$ and $A(2f_c)$ denote the spectral amplitude at the excitation frequency and at the second harmonic in the frequency domain. The variation of DI with crack damage intensity is shown for S0 and A0 packets in Figure 10a and for the new packet in Figure 10b. It can be observed in Figure 10 that the amplitude ratio DI is relatively small for both S0 and A0 packets, but it is quite big for the new wave packet even at small values of r. The DI for S0 and A0 has a monotonically increasing relationship with the crack damage intensity. So the ratio DI from the new packet could serve as an early indicator for the presence of a breathing crack, and the ratio DI for the S0 and A0 packets can serve as an indicator of damage severity. It should be noted that the damage index only depends on the ratio of frequency spectral amplitude; it does not require any baseline data. So this DI based on nonlinear guided wave is a baseline free indicator for damage presence and severity.

6. CONCLUSIONS AND FUTURE WORK

In this paper, predictive simulation of nonlinear Lamb wave interaction with a crack is carried out using finite element method (FEM). The breathing crack is modeled via the "element birth and death" technique, which is found to behave well with respect to opening and closing under tension and compression. The result shows the "element birth and death" method is capable of simulating a breathing crack.

Besides S0 and A0 packets, a new packet is observed in the time domain signal due to the presence of the breathing crack. The nonlinear phenomenon of higher harmonics can be noticed in the frequency spectrum all the wave packets. This distinctive feature allows us to tell the presence of cracks initiated in structure components. Different cases with various damage severities are investigated and compared. A baseline free damage index is proposed based on higher harmonics amplitude. This damage index is found to increase monotonically with damage for the S0 and A0 wave packets. However, for the new wave packet, this damage index is very sensitive to low damage values, but does not increase thereafter. Using this damage index, we find that the new packet is more sensitive to the presence of the crack, while S0 and A0 packets can provide monitoring information on the severity of damage growth.

Future work on this nonlinear study should include theoretical models to simulate nonlinear wave propagation in 3D plate structures. Different causes of nonlinearity should also be investigated like nonlinear material properties, PWAS nonlinearity, bolted lap-joints, etc. Experimental work should be carried out to verify these theoretical predictions and apply the nonlinear behavior to structural health monitoring and non-destructive evaluation.

7. ACKNOWLEDGEMENTS

Support of Office of Naval Research # N00014-11-1-0271, Dr. Ignacio Perez, Technical Representative; Air Force Office of Scientific Research #FA9550-11-1-0133, Dr. David Stargel, Program Manager; are thankfully acknowledged.

REFERENCES

[1] Jhang, K. Y., "Nonlinear Ultrasonic Techniques for Non-linear destructive Assessment of Micro Damage in Material: A Review", International journal of precision engineering and manufacturing. Vol.10 Issue: 1, 123-135 (2009)

[2] Kruse, W.; Zagrai, A. N. , "Investigation of Linear and Nonlinear Electromechanical Impedance Techniques for Detection of Fatigue Damage in Aerospace Materials", 7th International Workshop on Structural Health Monitoring, Stanford Univ. , CA, 9-11 Sept. (2009)

[3] Donskoy, D.; Reznik, A.; Zagrai, A.; Ekimov, A., "Nonlinear Vibrations of Buried Land Mines", Journal of the Acoustical Society of America (JASA), Vol. 117, N. 2, 690-700 (2005)

[4] Adler, L.; Rokhlin, S. I., "Parametric Resonance for Material Characterization", CP1096 Review of Quantitative Nondestructive Evaluation, Vol. 28, D. O. Thompson and D. E. Chimenti (Eds.), AIP 2009, 238-245 (2009)

[5] Viswanath, A.; Rao, B. Purna, C.; Mahadevan S., "Nondestructive assessment of tensile properties of cold worked AISI type 304 stainless steel using nonlinear ultrasonic technique", Journal of materials processing technology Vol. 211, Issue 3, 538-544 (2010)

[6] Nagy, P. B., "Fatigue Damage Assessment by Nonlinear Ultrasonic Materials Characterization", Ultrasonics, Vol. 36, 375-381 (1998)

[7] Hermann, J.; Jacobs, L. J.; Qu, J.; Kim, J-Y "Generation and detection of higher harmonics in Rayleigh waves using laser ultrasound", CP820 Review of Quantitative Nondestructive Evaluation, Vol. 25, D. O. Thompson and D. E. Chimenti (Eds.), AIP 2006, pp. 262-269 (2006)

[8] Bermes, C.; Kim, J. Y.; Qu, J., "Experimental characterization of material nonlinearity using Lamb waves", Applied physics letters Vol.90, Issue 2 Article Number: 021901 DOI: 10.1063/1.2431467 (2007)

[9] Xiang, Y.X.; Deng, M.X.; Xuan, F.Z., " Cumulative second-harmonic analysis of ultrasonic Lamb waves for aging behavior study of modified-HP austenite steel", Ultrasonics Vol. 51, Issue 8, 974-981 (2011)

[10] Lee, T. H.; Choi, I. H. "The Nonlinearity of Guided Waves in an Elastic Plate", Modern Physics Letter Series B, 22(11), 1135-1140 (2008)

[11] Deng, M.X., "Analysis of second-harmonic generation of Lamb modes using a modal analysis approach", Journal of applied physics Vol. 94, Issue 6 , 4152-4159 (2003)

[12] Deng, M.X., "Cumulative second-harmonic generation of Lamb-modes propagation in a solid plate", Journal of applied physics Vol. 85, Issue: 6, 3051-3058 (1999)

[13] Dutta, D.; Sohn, H.; Harries, K. A., " A nonlinear acoustic technique for crack detection in metallic structures", Structural Health Monitoring-an international journal Vol. 8, Issue: 6, 573-573 (2009)

[14] Cantrell, J. H , "Nondestructive Evaluation of Metal Fatigue Using Nonlinear Acoustics", CP1096 Review of Quantitative Nondestructive Evaluation, Vol. 28, D. O. Thompson and D. E. Chimenti (Eds.), AIP 2009, 19-32 (2009)

[15] Kumar, A.; Torbert, C.; Jones, J. W.; Pollock, T. M. "Nonlinear Ultrasonics for In Situ Damage Detection during High Frequency Fatigue", Journal of Applied Physics, Vol. 106, 024904_1-9 (2009)

[16] Andreaus, U.; Casini, P.; Vestroni, F., " Non-linear dynamics of a cracked cantilever beam under harmonic excitation", International journal of non-linear mechanics Vol. 42, Issue 3, 566-575 (2007)

[17] Bouboulas A. S.; Anifantis N. K., "Finite element modeling of a vibrating beam with a breathing crack: observations on crack detection", Structural Health Monitoring-an international journal Vol. 10, Issue 2,

131-145 (2011)

[18] Okada, J; Ito, T; Kawashima, K., "Finite element simulation of nonlinear acoustic behavior at minute cracks using singular element", Japanese journal of applied physics part 1-regular papers short notes & review papers Vol. 40, Issue 5B, 3579-3582 (2001)

[19] Nakahata, K.; Hirose, S., "Simulation of Nonlinear Ultrasonic Wave Through an Interface Including Imperfections", CP820 Review of Quantitative Nondestructive Evaluation, Vol. 25, D. O. Thompson and D. E. Chimenti (Eds.), AIP 2006, 270-276 (2006)

[20] Giurgiutiu V., [Structural Health Monitoring with Piezoelectric Wafer Active Sensors], Academic Press, 747 pages, ISBN 9780120887606 (2007)

[21] Hagedorn, P. [Nonlinear Oscillations], Oxford Univ. Press, New York, 3-54 (1978)

[22] Naugoslnykh, K; Ostrovsky, L. [Nonlinear Wave Processes in Acoustics], Cambridge Univ. Press, Cambridge, MA, (1998)

[23] Norris, A. N. [Finite Amplitude Waves in Solids in Nonlinear Acoustics], Hamilton, M. F; Blackstock, D. T. (Eds.) Academic Press, New York, (1998)

[24] Ostrovsky, L. A.; Potapov, A. S. [Modulated Waves], The John Hopkins Univ. Press, Baltimore, MD, (1999)

[25] Jhang, K. Y., "Applications of Nonlinear ultrasonics to the NDE of Material degradation", IEEE transactions on ultrasonics ferroelectrics and frequency control Vol. 47, Issue 3, 540-548 (2000)

[26] Giurgiutiu, V., "Current Issues in Vibration-Based Fault Diagnostics and Prognostics", SPIE's 9th Annual International Symposium on Smart Structures and Materials and 7th Annual international Symposium on NDE for Health Monitoring and Diagnostics, 17-2 march 2002, San Diego, Ca. paper # 4702-15 (2002)

[27] ANSYS 13.0 Help. Chapter 13: Element Birth and Death.

[28] Long, R. S.; Liu, W. J.; Xing, F., " Numerical simulation of thermal behavior during laser metal deposition shaping", Transactions of nonferrous metals society of china Vol. 18, Issue 3, 691-699 (2008)

[29] Giurgiutiu, V. "Tuned Lamb wave excitation and detection with piezoelectric wafer active sensors for structural health monitoring", Journal of intelligent material systems and structures Vol. 16, Issue 4, 291-305 (2005)